INL/CON-18-52041-Revision-1

MCNP AND CFD MODELING OF A SODIUM FAST REACTOR SUB-ASSEMBLY CHANNEL TO CAPTURE LOCALIZED TEMPERATURE PEAKING

Abdalla Abou Jaoude, Su Jong Yoon, Samuel E Bays

June 2019

The INL is a U.S. Department of Energy National Laboratory
operated by Battelle Energy Alliance

INL/CON-18-52041-Revision-1

MCNP AND CFD MODELING OF A SODIUM FAST REACTOR SUB-ASSEMBLY CHANNEL TO CAPTURE LOCALIZED TEMPERATURE PEAKING

Abdalla Abou Jaoude, Su Jong Yoon, Samuel E Bays

June 2019

Idaho National Laboratory
Idaho Falls, Idaho 83415

http://www.inl.gov

Prepared for the
U.S. Department of Energy

Under DOE Idaho Operations Office
Contract DE-AC07-05ID14517

MCNP AND CFD MODELING OF A SODIUM FAST REACTOR SUB-ASSEMBLY CHANNEL TO CAPTURE LOCALIZED TEMPERATURE PEAKING

A. Abou-Jaoude[1], S-J. Yoon[1], and S. E. Bays[1]

[1]Idaho National Laboratory
2525 Fremont Ave., Idaho Falls, ID 83415

abdalla.aboujaoude@inl.gov, sujong.yoon@inl.gov, samuel.bays@inl.gov

ABSTRACT

Typical evaluation tools for sodium-cooled fast reactors (SFR) use simplified neutronic/thermal models to efficiently compute the power and temperature distributions within the core. However, their modeling capability can be limited in extreme cases such as when sharp inter-assembly power gradients occur, or for non-standard SFR assembly geometries. Higher fidelity tools that rely on Monte Carlo methods for neutron transport, and Computational Fluid Dynamics (CFD) for thermal analysis, are better suited in these instances. The higher accuracy comes at the cost of higher computational expense. MCNP and STAR CCM+ were selected for this analysis. While MCNP is capable of generating pin-level power distributions for a whole-core SFR model, it is prohibitively expensive to then conduct CFD analysis for every single assembly. A simple model was therefore developed to rapidly estimate pin temperature distributions throughout the whole core for scoping calculations. It relies on the application of a polynomial function to correct the temperatures obtained using a 1-D heat balance equation assuming independent channels. The polynomial function is obtained from a CFD simulation of a single fuel assembly with a uniform power distribution and an adiabatic boundary condition. Without using CFD, each sub-channel outlet temperature is calculated separately using 1-D heat-balance and the MCNP calculated pin-powers. The rudimentary 1-D model is then corrected for the flow-mixing effect based on the CFD data. The temperature calculation is performed by a code written in the Python language called CFD Monte-Carlo Developed Reconstruction of Sub-channel at a Quasi-Representative Level (CMDR-SQRL). CMDR-SQRL was shown to adequately predict CFD evaluated temperature distribution for a wide range of SFR configurations, including an extreme case with fuel assemblies nearby containing moderating material. The agreement demonstrates how geometric and power-distribution-driven effects can be decoupled within an SFR assembly. CMDR-SQRL is intended to be mainly used for scoping studies to provide core-wide evaluations efficiently.

KEYWORDS: sodium fast reactor, power peaking, flow mixing, CFD, neutron transport

1. INTRODUCTION

Typical analysis of Sodium-cooled Fast Reactors (SFR) relies on nodal neutronics codes and simplified thermal hydraulics models. These tools are very suitable for use in the fast neutron spectrum and for single-phase flow analysis. The neutronics codes are usually based on variational nodal methods (e.g.

DIF3D/VARIANT [1]), while thermal codes rely on simplified sub-channel heat transfer models (e.g. SuperEnergy-2 [2]). The neutron transport simulations can provide detailed power profiles within the assembly. The sub-channel codes are then needed to determine the corresponding temperature profile and account for geometry-driven (i.e., turbulent mixing and channel dependent flow areas) temperature variations within an assembly.

Higher fidelity codes tend to be computationally intensive and provide little gains in accuracy for standard SFR analysis. The main exception is when large heterogeneities are introduced within an SFR core resulting in significant variations in spectrum or sharp changes in total flux. The nodal approximations are unable to capture the sharp gradients observed at such interfaces. In those instances, Monte Carlo based neutron transport codes such as MCNP are better suited [3].

With regards to thermal hydraulic modeling, while the sub-channel codes tend to yield adequate results in SFR analysis, they also tend to be limited for very specific geometries. Computational fluid dynamics (CFD) codes can provide higher-fidelity evaluations and are less restricted in terms of geometric features. CFD codes can explicitly model intra-channel heat/mass exchanges and turbulent flow mixing effects, rather than relying on empirical correlations as is typically done in sub-channel codes. For example, in the SUPERENERGY-II code, the swirl induced turbulent mixing is modelled with the eddy-diffusivity correlation [4]. Finite Volume Method (FVM)-based CFD code, STAR CCM+ ver.12.06.011-R8 was selected as the numerical solver in this study [5].

It is hypothesized that the dominant turbulent mixing effect is caused by the presence of the SFR fuel pin wire-wrap, and that this "swirl mixing" is separable from mixing caused by any lateral pressure differential across the fuel assembly. Therefore, the turbulent mixing effect can be analyzed as a 'geometry' effect, not a nuclear effect. It is proposed to leverage a single CFD fuel assembly simulation to provide high fidelity data to then augment a low fidelity 1-D channel code based on the assumption that power and geometry-driven temperature variations can be superimposed. In this scheme, geometric swirl mixing effects would only need to be evaluated once using CFD for a given assembly type. The CFD derived fuel assembly outlet temperature distribution is then used to derive a correction factor to apply to the 1-D channel code. The CFD Monte-Carlo Developed Reconstruction of Sub-channel at a Quasi-Representative Level (CMDR-SQRL) code estimates the outlet sodium temperature in each pin-channel separately, then corrects the value using the CFD derived correction factor. The correction factor is a function of radial distance from the center of the fuel assembly. Once pin-level power generation is obtained by MCNP, CMDR-SQRL then rapidly generates a first order estimate of temperature distributions across the core rather than having to rely on CFD simulations for every assembly. In this work, the proposed methodology is verified against CFD models for a standard SFR power distribution, and a more extreme case in order to highlight its capabilities.

2. PROPOSED METHODOLOGY

2.1. Neutron Transport and Computational Fluid Dynamics

Monte Carlo Nth Particle, v6.1 (MCNP) was selected for the neutron transport simulations [3]. SFR geometry including fuel pins can be modeled explicitly in order to gain a higher level of accuracy. Fission energy release is tallied at each individual fuel rod and axially integrated. The MCNP +F6 collisional heating tally was used. This tally type combines fission product energy deposition with collisional heating from all tracked secondary particles. In this case, both neutrons and photons were tracked. Thus, in the calculation only fission product energy is deposited locally at the fission site. Prompt neutron and gamma ray kinetic energy is carried away from the fission site and deposited throughout the reactor geometry as collisional heating. Secondary particles are also tracked and contribute to collisional heating.

For the current coolant channel analysis, only the fission product and collisional heating within the fuel meat is considered. Future works will include collisional heating within the cladding and coolant as well. All assemblies are assumed to contain fresh fuel for the purpose of this analysis. Sufficient particle histories were simulated to ensure a reactivity standard deviation less than 20 pcm and a pin power uncertainty less than 1%. An example SFR pin-level power distribution is shown in Figure 1.

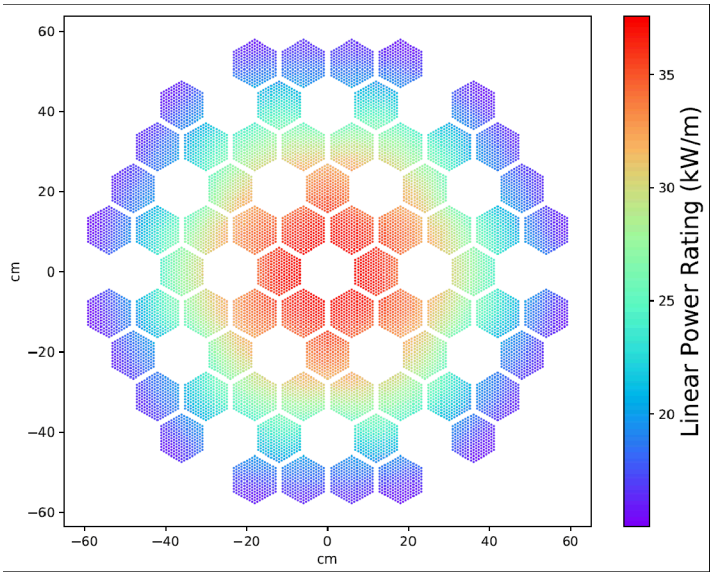

Figure 1. MCNP whole-core power tally results for an SFR showing linear power rating at individual fuel pins.

The pin-level power generation data is then used for thermal analysis. A three-dimensional CFD model of a wire-wrapped SFR fuel assembly was developed as seen in Figure 2. Steady-state, incompressible, Reynolds-Averaged Navier-Stokes (RANS) equations are solved by adopting the segregated flow, segregated flow temperature and Shear Stress Transport (SST) k-ω turbulence model with all y+ wall treatment [6]. The computational domain was meshed by the polyhedral mesh with the prism boundary layer mesh. Previous studies showed that the number of mesh for wire-wrapped fuel assembly can be reduced by elongating computational cells in a streamwise direction without distorting the results when the aspect ratio is less than 8:1 [7] [8]. The aspect ratio of cell used in this study was 4:1. Average wall y+ value of heated wall was approximately 12.4. Total number of mesh cells was 92 million. The wall boundary condition was assumed to be adiabatic.

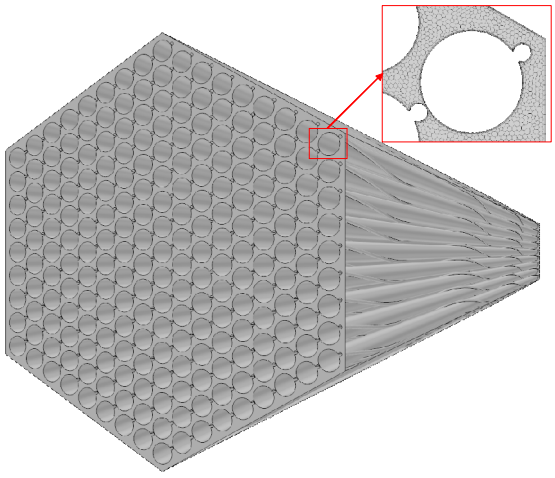

Figure 2. CFD model of 217-pin Wire-Wrapped Fuel Assembly.

2.2. Simplified Sub-Channel Analysis Tool

SFR fuel pin-lattices are enveloped in a hexagonal duct. Unlike light water reactors, which use grid-spacers at various axial levels, separation of SFR pins is provided by a wire that is spirally wrapped around the fuel pin. Because of wire-wrap and duct arrangement, the channel flow area between the outer row of fuel pins and the hexagonal wall is greater than that for channels within the pin-lattice itself. Therefore, the coolant temperature is lower nearer the wall due to the higher coolant mass flow in that region. The use of a duct prevents crossflow between fuel assemblies. Therefore, any intra-assembly crossflow is only due to intra-assembly power gradients. However, the helical wire wrap does induce turbulent mixing absent of lateral mass transfer. The result of the mixing is that thermal energy is rebalanced within the fuel assembly as the coolant travels through it. The turbulent mixing effect has little impact on the magnitude of the hot-channel temperature, i.e., the center pins within a fuel assembly. It does, however, create a smoothing effect on the channel temperatures in the outer regions of the fuel assembly, i.e., between channels with interior flow area and those with a greater flow area due to their proximity with the duct wall. The variation between the center and wall temperature due to turbulent mixing effects is well characterized by Memmott et al. [9].

The methodology followed in the analysis of temperature peaking effects due to swirl flow is summarize in Figure 3. Fuel pin level MCNP fission power tallies were extracted by CMDR-SQRL and used to compute thermal outlet conditions using simplified 1-D models. Standard heat balance equations, $q = \dot{m}C_p\Delta T$, are used for channel temperature rise. CMDR-SQRL then biases the channel outlet temperature using a correction factor generated from CFD analysis.

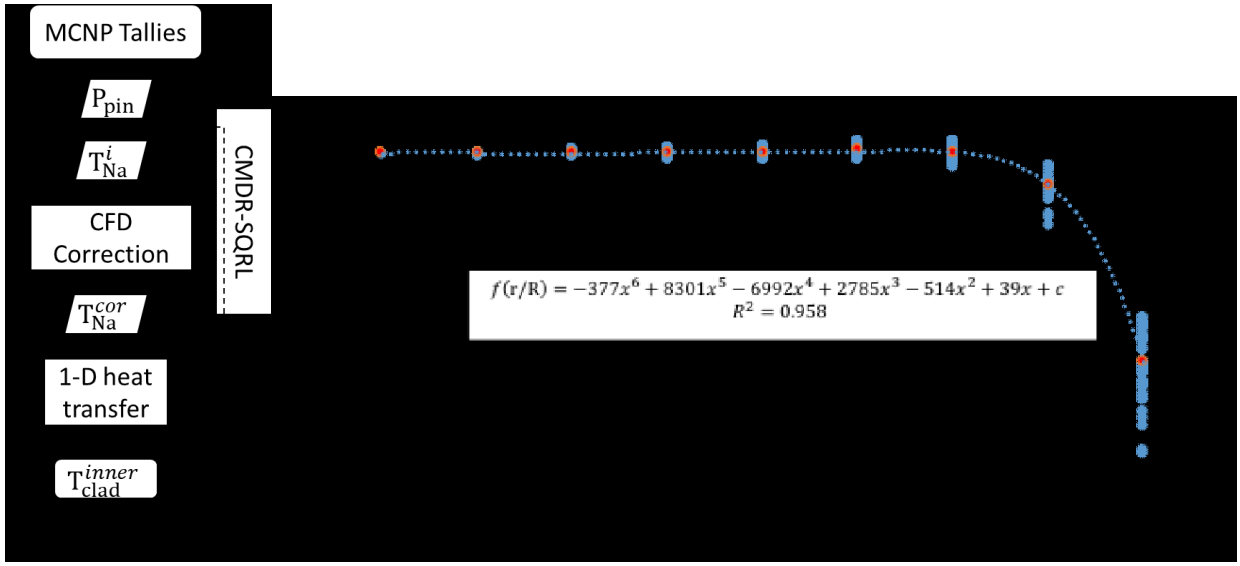

Figure 3. Flow diagram for thermal calculation (left), temperature drop correlation curve inside of a given SFR assembly (right). Blue dots represent each fuel pin the assembly, red data points are the averages at each radial position, highlighting the good agreement with the polynomial fit.

The correction factor is derived from a single standalone CFD model of a fuel assembly having average power and flow for the SFR. All fuel pins are modelled at the same uniform average power. The model assumes an adiabatic boundary condition. As shown in Figure 4, the swirl flow effect tends to smooth out the temperature distribution in the outer two fuel rows. The curve in Figure 3 represents the temperature profile of Figure 4 collapsed into a 1-D format.

A 6th order polynomial was used to determine the effect on , $T_{surface} - T_{inlet}$, across the length of a channel.

As shown in Figure 3, the fitted curve agrees well with the CFD result at each radial position. Because the polynomial, f, is fitted against CFD cladding surface temperatures, thermal boundary layer effects are accounted in addition to swirl mixing. The parameter represents the distance to the wall for a given azimuthal angle. The large variability observed in the CFD outer-row pin temperatures is due to swirling effects within the assembly.

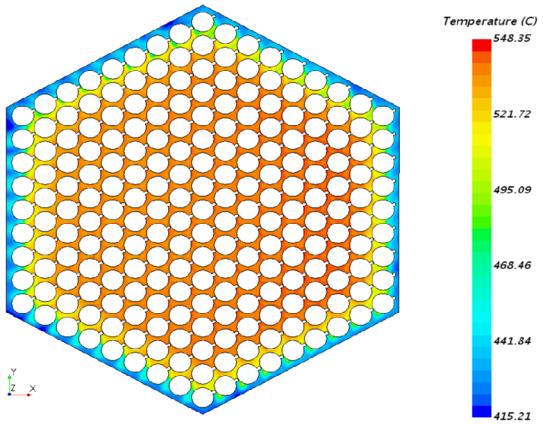

Figure 4. CFD outlet sodium temperature inside an assembly with a uniform power distribution.

The fitting curve *is* then integrated and normalized to zero in order to determine the value of parameter in Equation 1 below. This ensures that the correction factor conserves energy and maintains the same fuel assembly average coolant outlet temperature. As a result, a value of 11.51 was selected.

(1)

The correction factor is then incorporated into following the two relations below. $\Delta T_{1D,i}$ is the initial

estimate for the temperature rise across a channel based on the 1-D model. The pin power, P_i, the fuel

pin average mass flow rate per pin, $\dot{m}_i$, and the average sodium heat capacity, , are needed for this initial

estimate. It is important to note that there is no sub-channel "mesh" associated with this method. Each fuel pin is associated with one heated pipe-like structure with flow area associated with the pin-cell. The coolant mass flow for this pipe is the mass flow for the entire fuel assembly divided by the total number of fuel pins and scaled in proportion to the ratio of flow area among the pin-lattice per total flow area within the assembly duct. This value A_{ratio}, is considered constant for every fuel pin-cell. Variations in flow area in the physical system are accounted for via the CFD model.

(2)

The CFD derived correction factor is then applied for a given pin position, , to correct for swirl flow

effects, thus giving $\Delta T_{Corr,i}$. The methodology relies on the assumption that there is no appreciable transverse cross-flow (i.e., power gradient driven) and that all mixing effects are due to swirl flow (ie., wire wrap geometry driven). This will be verified in the analysis of Section 3. It should be noted that while $\Delta T_{1D,i}$ corresponds to bulk channel sodium, $\Delta T_{Corr,i}$ corresponds to the pin surface temperature. Boundary layer effects are accounted for in the CFD model.

(3)

After the corrected surface sodium temperature (i.e., cladding outside temperature) is found, a 1-D radial heat transfer analysis is conducted to solve for the fuel cladding inside temperature at the core outlet. This is a key performance metric for SFR metallic alloy fuel in steel cladding because this is the location for which the fuel is most susceptible to Fuel-Cladding-Chemical-Interaction (FCCI). Equation 4 shows the method for computing the fuel cladding inside temperature.

(4)

The cladding surface temperature at channel exit is the sum of the coolant inlet temperature, T_{inlet}, and the result of Equation 3. The Linear Heat Generation Rate of fuel pin i, $LHGR_i$, is taken to be at the top of the fuel pin, z=H, where the bulk sodium coolant temperature is greatest. R_{co} is the outer radius of the fuel pin. R_{ci} is the insider radius of the fuel pin. Sodium properties used in this work, are computed using temperature dependent fitting curves [10]. k_{clad} is the thermal conductivity of the cladding alloy assumed to be HT9 [11].

FCCI in metallic alloy SFR fuels occurs when cladding constituents diffuse into the fuel slug to form a lower melting-point alloy at the fuel/cladding interface. The degree of formation of this intermetallic layer is proportional to burnup. If the cladding inside temperature exceeds the eutectic melting temperature for this intermetallic layer, such as in an off-normal condition, a liquid layer is formed that

propagates through the cladding until it is breached. The rate of cladding "wastage" due to eutectic melting is proportional to the degree of burnup and the cladding inside temperature. The threshold for eutectic melting is limited to 650°C at 11% Fission per Initial Metal Atom (FIMA) [12]. On average, the inside cladding temperature is 16°C is hotter than the bulk sodium coolant around it.

3. APPLICATION AND VERIFICATION

3.1. Standard SFR Core Layout

In light of the recent interest in the U.S. to re-establish a SFR test reactor capability, an SFR model loosely based on current Versatile Test Reactor (VTR) scoping studies is selected as a test case for the proposed methodology [13]. This test case is shown in Figure 5. The reactor is sodium-cooled, employs a metallic fuel (blue assemblies), and is rated at 300 MW_{th}. The locations specified in orange are non-fuel locations for either control assemblies or test locations. Since this level of detail is not needed for this study, they are not specified in this paper. Section 3.2 will consider experiments that are limiting to assess using standard tools. In this section, these test assemblies are modeled as empty sodium channels. The fuel assembly dimensions for the models are summarized in Table I. The assemblies were assumed to have three different flow orifices. The flow through a fuel assembly in the first two fuel rings is assumed to be 31.9 kg/s. The flow in the fourth ring is 26.5 kg/s, and 20.7 kg/s in the last two rows.

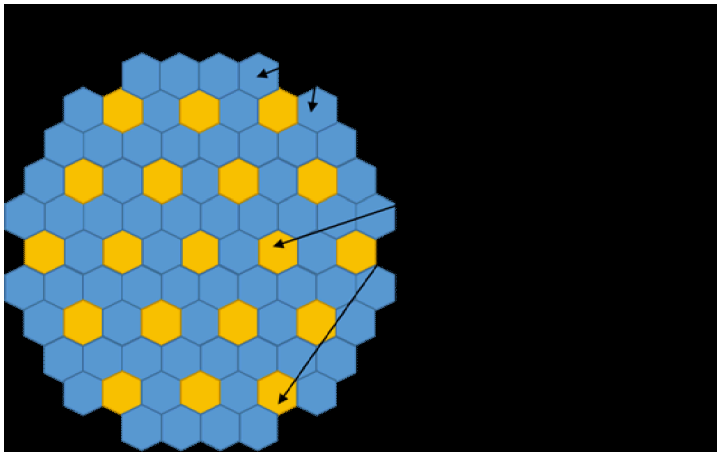

Figure 5. Diagram of the considered core configurations.

Table I. Assembly dimensions and specifications.

Pin diameter	0.625 cm
Wire wrap diameter	0.110 cm
Clad thickness	0.045 cm
Assembly pitch	12.0 cm
Inner flat-to-flat	11.1 cm
Fuel length	80.0 cm
Number of rods	217

MCNP was used to tally the pin power distributions. The results were previously shown in Figure 1. CMDR-SQRL was then used to generate temperature distributions across the whole core. CFD analysis for 66 fuel assemblies is prohibitively expensive, therefore the verification was conducted for a line C-C' across the core. A comparison of the results is shown in Figure 6. The radial power distribution of pins

nearest to line C-C' is also shown. The compelling conclusion from Figure 6 is that not only the fuel assembly with power gradient matching closest to the uniform distribution FA(-1, 1) agrees, but the fuel assembly with the steepest radial power gradient FA(-1, 4) also agrees to the same level of precision.

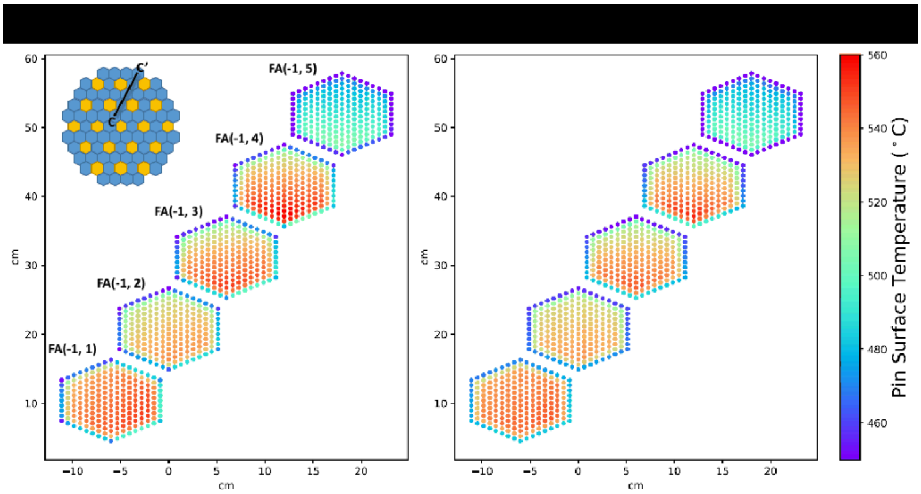

Figure 6. Comparison of CFD versus CMDR-SQRL results for the pin surface temperature at coolant channel exit along the section C-C' of the core.

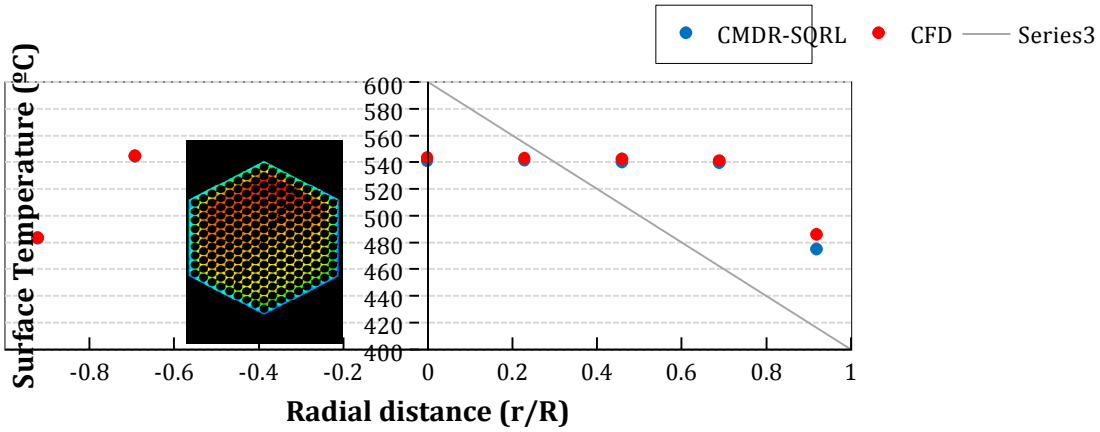

Figure 7. Differences in predicted outlet surface temperature along the A-A' line of FA(-1, 1).

Figure 7 above shows a close-up of temperature variations across fuel assembly FA(-1, 1). The plot shows the radial outlet surface temperature profiles in FA(-1, 1) across the A-A' section (60º angle). The results agree very well, with most temperature value seeing a deviance of 0.3%, while the largest deviance is no more than 2.3%. The larger deviance at the edge pin can be attributed to the large variability in edge temperature previously highlighted in Figure 3. This could potentially be addressed in future work if the fitting function accounts for azimuthal variations in temperature alongside radial ones.

3.2. Heterogeneous SFR Core Configuration

While the design basis of the VTR is limited to only fast spectrum tests, there is precedence for moderator-filled tests in previous fast test SFRs. A moderated test is considered for this work solely on the basis that it offers the most extreme challenge to the method described in Section 2. Both the Fast Flux Test Facility (FFTF) in the United States of America and the Phénix Reactor in France had experimented with

such assemblies. The FFTF moderated experiments, contained a lattice of Yttrium-Hydride rods and isotope target pins. The Cobalt Test Assembly (CTA) demonstrated medical isotope production, i.e., Co-60 as well as Gd-153 [14]. The CTA was irradiated in 1986. A later FFTF moderated test, called the Multi-Isotope Production Test Assembly (MIP), was used to measure nuclear data uncertainties for various isotopes. The MIP was irradiated in 1989 [15]. The Phenix ECRIX experiments consisted of an annulus of CaH_2 (called ECRIX-H) or depleted boron in $^{11}B4C$ (called ECRIX-B) surrounding a single pin containing minor actinides [16] [17] [18]. The main goal of the ECRIX tests were to moderate the fast neutron spectrum to maximize minor actinide transmutation. These two experiments were irradiated successfully in the Phénix reactor between 2003 and 2006. To test CMDR-SQRL's capability under an extreme scenario that is difficult to model using standard SFR analysis tools, the PHENIX ECRIX-B test was considered for the model [16], [17]. It contains depleted B_4C as moderating material, with zero-to-low ^{10}B content to ensure no neutron poisoning. Within the cylindrical shroud of moderating material is a single fuel pin. The fuel test is made of a CERCER of dispersed AmO_2-MgO contained within MgO [19].

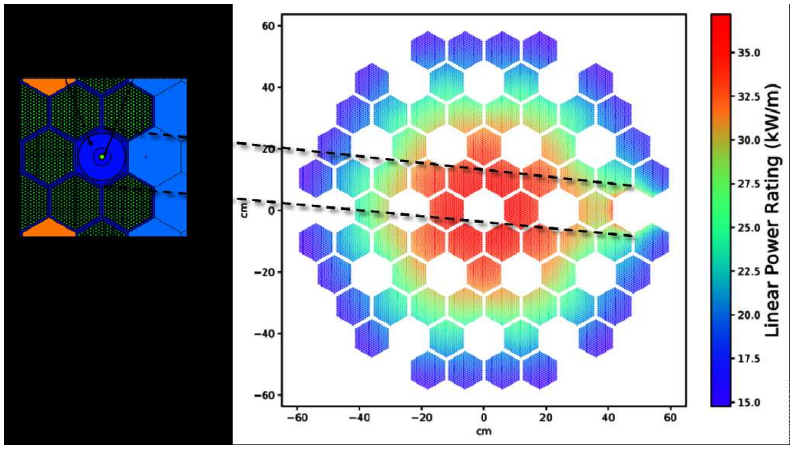

Figure 8. Illustration of the ECRIX experiment (left) inserted into row 5. Depleted boron is used as the moderating material, with less than 1% 10B content. Pin-level power generation in the SFR model (right) with the ECRIX-B experiment loaded in the easternmost test position

The moderated-test as modeled inside the core model is shown in Figure 8 (above) with the resulting pin-power distribution obtained from MNCP6. Notable localized peaking can be observed in the pins adjacent to the test. As expected, the power peaking is limited to the two rows of fuel pins nearest to the moderated experiment. This is in light of the reduced mean free paths of thermalized neutrons traveling back from the experiment into the fuel assembly. The outlet fluid temperatures of fuel assemblies adjacent to the experiment in the CFD simulations are shown, Figure 9. Although the peak fuel pin power of FA(4,-1) was lower than that of FA(3,0), the core peak fluid temperature is observed in FA(4,-1) because it belongs to the third orifice zone, where the mass flow rate is lowest.

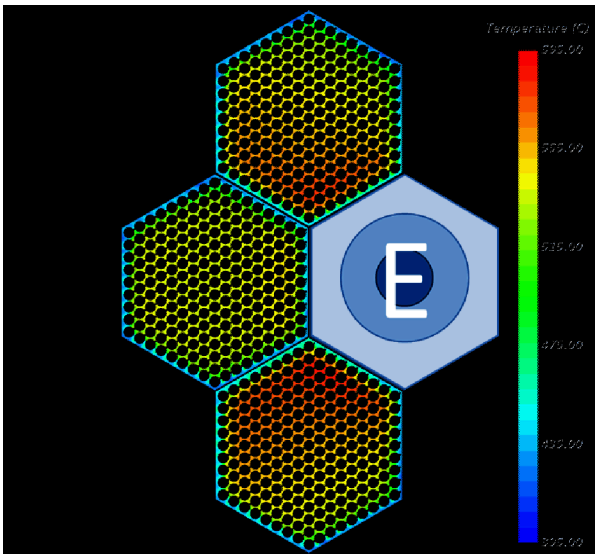

Figure 9. Outlet fluid temperature distribution computed by CFD analysis for assemblies adjacent to the ECRIX experiment (labeled 'E').

Figure 10 shows the peak inner clad temperatures at the vicinity of the experiment. It can be seem that all values are below the FCCI threshold, 650ºC [12]. The surface pin temperature was then compared between CMDR-SQRL and the CFD models. Figure 11 provides a zoomed-in view of assembly FA(4, -1) (south-west of the ECRIX test). Relatively good agreement is observed again between the two models, thus verifying the methodology for cases with sharp power gradients.

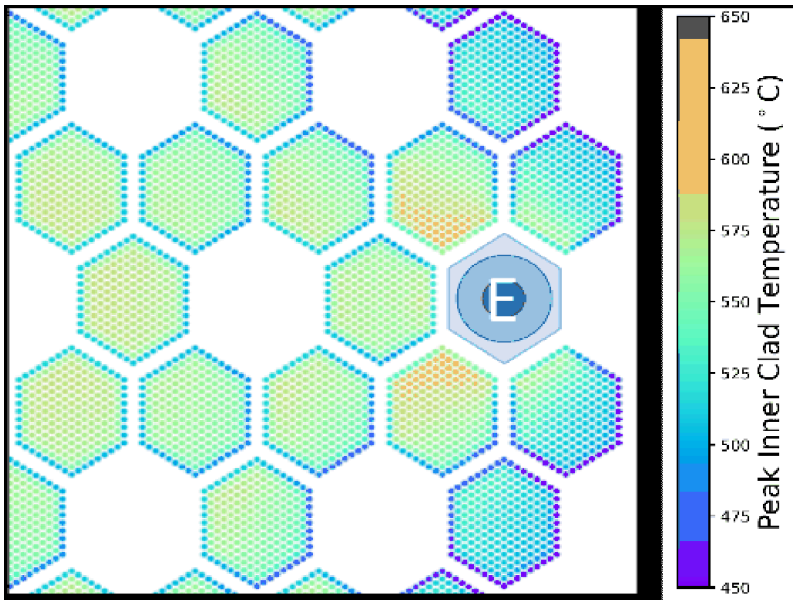

Figure 10. Inner clad temperatures computed with CMDR-SQRL. The assembly marked with an 'E' represents the ECRIX experiment position.

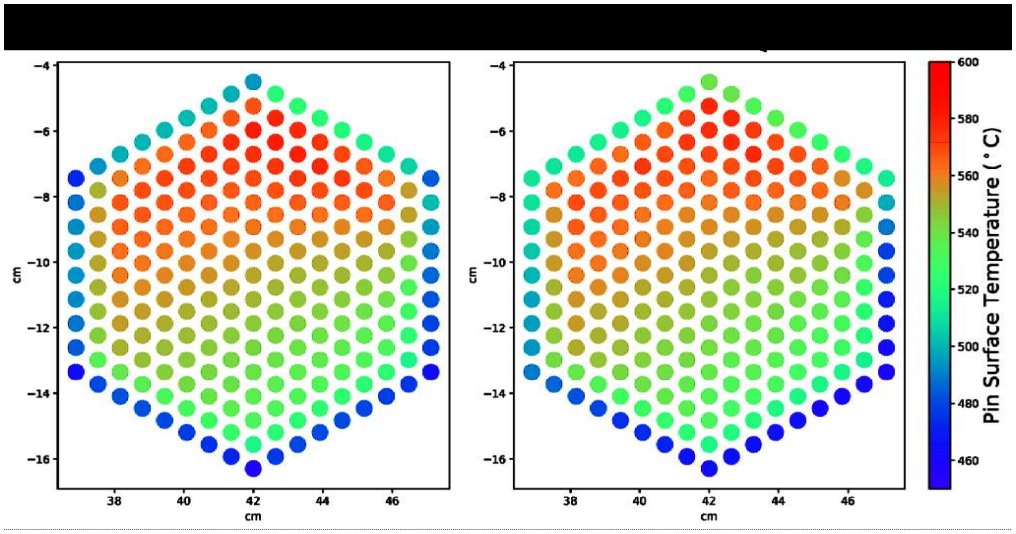

Figure 11. Comparison of pin surface temperature estimates for FA(4, -1) using CFD or CMDR-SQRL.

A close-up of the variation within assembly FA(4, -1) is provided in Figure 11 across the A-A' section (60º angle). The ECRIX test is located in the +x direction. The resulting deviance between the two models is still within the 2% range as observed in Section 3.1. The results show the importance of accounting for geometric mixing effects in outer row pins. Serendipitously, the heat transport due to swirl mixing, and driven by the greater flow area between outer row pins and the duct wall, provides over-cooling in the two outer fuel pin rows that have the most pronounced power peaking due to the moderated test.

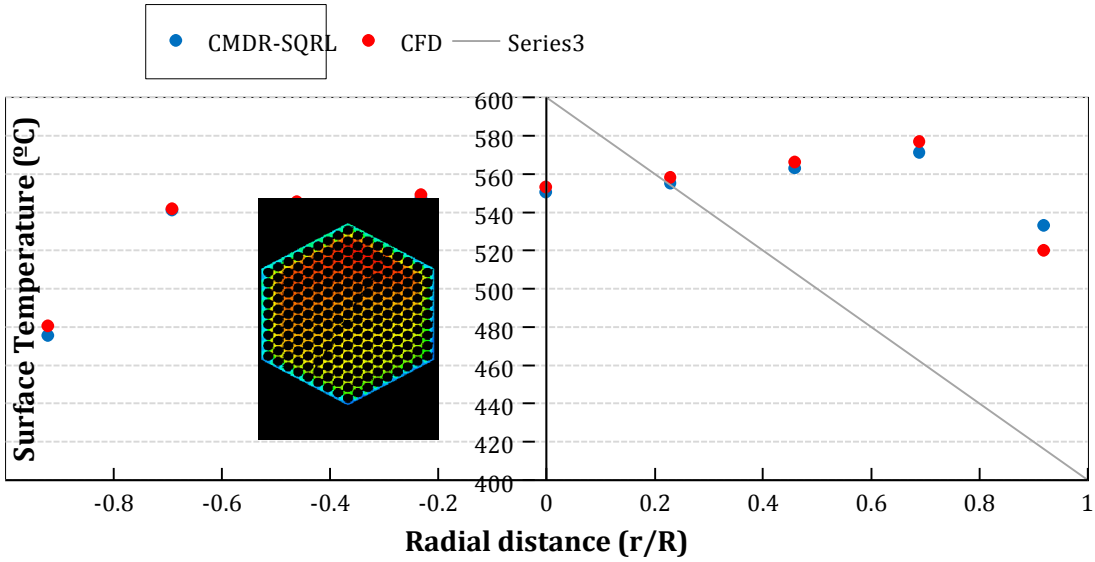

Figure 12. Comparison of the radial pin surface temperature across A-A' for FA(4, -1).

Table II summarizes the results for the three assemblies adjacent to ECRIX that saw the most pronounced power peaking. Peak surface temperatures agree to within 4°C, while average temperatures agree within 1-2°C. This is considered to be sufficiently close for employing CMDR-SQRL as an initial scoping tool for considering different experiment configurations inside a fast test reactor.

Table II. Comparison of pin surface temperatures in assemblies near the ECRIX-B experiment.

	CFD		CMDR-SQRL		
Assembly Position	**Average Surface Temperature**	**Peak Surface Temperature**	**Average Surface Temperature**	**Peak Surface Temperature**	**Peak Inner Clad Temp.**
(3, 0)	525.1ºC	549.3ºC	523.6ºC	545.4ºC	575.0ºC
(3, 1)	537.4ºC	581.2ºC	537.0ºC	577.4ºC	604.1ºC
(4, -1)	538.1ºC	580.5ºC	537.5ºC	577.3ºC	605.3ºC

4. CONCLUSIONS

The analysis conducted confirmed the assumption that geometry-driven "swirl" is the dominant turbulent mixing effect when analyzing a SFR assembly. A simple low-order thermal hydraulic methodology was proposed for scoping studies using results from a single high-order fuel assembly CFD model. The coolant channel temperature data from this model is then used to solve for a polynomial function of temperature corrections. These temperature corrections are then used to adjust the coolant temperatures from a simple 1-D channel analysis calculation for every fuel pin in the SFR. Three-dimensional neutron transport simulations (e.g., MCNP) should be used to provide the pin power data to the 1-D channel analysis calculation. The proposed method is essentially a low-order method corrected using information from a high-order method.

An "extreme" test case was considered, whereby a SFR test location was filled with spectral shifting material ($^{11}B_4C$). Traditional SFR codes would struggle to analyze these types experiments. Acceptable agreement between the proposed method (CMDR-SQRL) and CFD was reached, thus demonstrating the robustness of the scoping tool for rapid analysis of impacts on fuel temperature peaking due to nearby advanced experiments in fast test reactors.

ACKNOWLEDGMENTS

This research work was prepared for the U.S. Department of Energy, through the INL LDRD Program, under DOE Idaho Operations Office, contract DE-AC07-05ID14517. This research also made use of the resources of the High-Performance Computing Center at Idaho National Laboratory, which is supported by the Office of Nuclear Energy of the U.S. Department of Energy and the Nuclear Science User Facilities under the same contract.

REFERENCES

[1] M. A. Smith and a. et., "DIF3D-VARIANT 11.0, A Decade of Updates," Argonne National Laboratory, Chicago, IL, 2014.

[2] K. L. Basehore and N. E. Todreas, "SUPERENERGY-2: A Multiassembly, Steady-State Computer Code for LMFBR Core Thermal-Hydraulic Analysis," Pacific Northwest Laboratory, Richland, WA, 1980.

[3] Pelowitz, D. B.; et. al., "MCNP6 Usure's Manual, Version 1.0," Los Alamos National Laboratory, LA-CP-13-00634, 2013.

[4] S. K. Cheng and N. E. Todreas, "Hydrodynamic Models and Correlations for Bare and

Wire-Wrapped Hexagonal Rod Bundles-Bundle Friction Factors, Subchanel Friction Factors and Mixing Parameters," *Nuclear Engineering and Design,* vol. 92, no. 2, pp. 227-251, 1986.

[5] Siemens PLM Software, "STAR-CCM+ User guide," 2018. [Online]. Available: https://mdx.plm.automation.siemens.com/star-ccm-plus.

[6] F. R. Menter, "Two-equation eddy-viscosity turbulence modeling for engineering applications," *AIAA Journal,* vol. 32, no. 8, pp. 1598-1605, 1994.

[7] J. G. Smith, T. Akira, D. W. Pointer and P. F. Fischer, "Predictions in CFD simulations of wire-wrapped SFR fuel assemblies," in *Proceedings of ICAPP '09*, Tokyo, Japan, 2009.

[8] J. W. Fricano and E. Baglietto, "A quantitative CFD benchmark for Sodium Fast Reactor fuel assembly modeling," *Annals of Nuclear Energy,* vol. 64, pp. 32-42, 2014.

[9] Memmott, M.; et. al., "On the use of RELAP5-3D as a Subchannel Analsysis Code," *Nuclear Engineering and Design,* vol. 240, pp. 807-815, 2010.

[10] Fink, J. K.; Leibowitz, L., "Thermodynamic and Transport Properties of Sodium Liquid and Vapor," Argonne National Laboratory, ANL/RE-95/2, 1995.

[11] Leibowitz, L.; Blomquist, R. A., "Thermal Conductivity and Thermal Expansion of Stainless Steels D9 and HT9," *International Journal of Thermophysics,* vol. 9, pp. 873-883, 1988.

[12] Cohen, A. B.; et. al., "Fuel/Cladding Compatibility in U-19Pu-10Zr/HT9-Clad Fuel at Elevated Temperatures," *Journal of Nuclear Materials,* vol. 204, pp. 244-251, 1993.

[13] F. Heidet, G. Youinou, T. Fei, M. A. Smith, G. Palmiotti and S. Bays, "Tradeoff Studies for a Versatile Fast Spectrum Test Reactor," in *Pacific Basin Nuclear Conference*, San Francisco, CA, USA, 2018.

[14] Wootan, D. W.; et. al., "Analysis and Results of a Hydrogen-Moderated Isotope Production Assembly in the Fast Flux Test Facility," *Nuclear Science and Engineering,* pp. 150-156, 1989.

[15] Wootan, D. W.; et. al., "Isotope Production Test in the Fast Flux Test Facility," in *Transactions of the American Nuclear Society*, Washington D.C., 1990.

[16] Garnier, J. C.; et. al., "The ECRIX Experiments," in *Proceedings of Global 1999*, Jackson Hole, WY, 1999.

[17] D. Warin, "Putting Transmutation Targets to the Test," *CLEFS CEA,* no. 46, Spring 2002.

[18] Bejaoui, S.; et. al., "ECRIX-H Experiment: Synthesis of Post-Irradiation Examinations and Simulations," *Journal of Nuclear Materials,* vol. 415, 2011.

[19] Croixmarie, Y.; et. al., "Fabrication of Transmutation Fuels and Targets: the ECRIX and CAMIX-COHIX Experience," *Journal of Nuclear Materials,* vol. 320, pp. 11-17, 2003.

[20] N. E. Todreas and M. S. Kazimi, Nuclear Systems I: Thermal Hydraulic Fundamentals, Levittown, Pennsylvania: Taylor and Francis, 1990, p. 451.